

Anomalous Large Difference in Dipole Moment of Isomers with Nearly Identical Thermodynamic Stability

Alexey B. Nadykto* and Fangqun Yu

Atmospheric Sciences Research Center, State University of New York at Albany, 251 Fuller Road, Albany, New York 12203

Received: December 16, 2007; Revised Manuscript Received: March 13, 2008

Sulfuric acid is a primary atmospheric nucleation precursor, with the ability to form stable aqueous hydrogen-bonded clusters/complexes. The electrical dipole moment of such clusters/complexes is important for ion-induced nucleation, largely controlled by dipole–charge interaction of airborne ions with vapor monomers and pre-existing clusters. Although experiments typically trace a single lowest energy conformer at low temperatures, the present study shows that the immediate vicinity (<1 kcal mol⁻¹) of the global minima may be populated with a number of isomers of nearly identical spectral characteristics and drastically different dipole moments. The difference in the dipole moment of mono-, di-, and trihydrates of the sulfuric acid exceeds 1.3–1.5 Debyes (~ 50 – 60%), 1.4–2.6 Debyes (~ 50 – 90%), and 3.8–4.2 Debyes (~ 370 – 550%), respectively. Being driven by the temperature dependence of the Boltzmann distribution, the difference between the Boltzmann–Gibbs average dipole moment and the dipole moment of the most stable isomer increases with the ambient temperature, leading to large variations in the dipole–ion interaction strength, which may have important implications for the ion-mediated production of ultrafine aerosol particles associated with various climatic and health impacts.

1. Introduction

The effect of atmospheric aerosols on the Earth's climate is unambiguous. Atmospheric aerosols can affect the Earth radiation balance directly, by absorbing and scattering solar radiation, or indirectly by modifying cloud properties.¹ Individual molecules of nucleating vapours experience various transformations before they become a cloud drop. Uncountable pre-existing clusters are initially formed; however, only few will be able to overcome the potential barrier and grow further, continuously facing a threat of being scavenged by larger competitors. The formation of new viable embryonic droplets (nucleation) is critically important. The dominant constituent of condensable vapours in the atmosphere, water is incapable of self-nucleation. A strong correlation between the sulfuric acid concentration and nucleation intensity observed *in situ* gives us a clear indication of the H₂SO₄ involvement.² A simple, strong, and hazardous mineral acid, common pollutant and, at the same time, primary nucleation precursor, sulfuric acid does play a key role in the atmospheric nucleation. However, the actual nucleation mechanism/mechanisms remain elusive despite impressive progress in experiments and theory achieved in last decades.^{3–6}

One of the major nucleation mechanisms in the Earth's atmosphere, nucleation on ions^{7–12} is affected by the dipole moment of condensable monomers and pre-existing clusters⁹ whose involvement in strong short-ranged dipole–charge interaction with airborne ions increases nucleation rates by many orders of magnitude.

Being engaged with water and ammonia, gas-phase H₂SO₄ grows into hydrogen bonded H₂SO₄–H₂O complexes. The ability of free sulfuric acid to gather several water monomers around it has direct impact on nucleation rates. Hydrates stabilize nucleating vapors and thus suppress binary homogeneous nucleation; however, their stability coupled with high polarity

could be beneficial for ion-induced nucleation. In the presence of ambient ionization from natural or anthropogenic sources in nucleating vapours, the immediate impact of the cluster polarity is elevated production of ultrafine aerosol particles responsible for various adverse public health effects^{13,14} and aerosol indirect radiative forcing.¹

Molecular hydrate complexes have been detected in sulfate aerosols and their stability has been corroborated in experiments.^{15–18} In year 2004, the high polarity of H₂SO₄ hydrates was predicted by Natsheh et al.¹⁹ Two years later, this finding has received an experimental confirmation in the work of Leopold with co-authors,¹³ who have reported dipole moment of 3.05 debyes for the most stable isomer of hydrogen-bonded (H₂SO₄)(H₂O) at $T = 3$ K.

The rigorous theoretical treatment of cluster microphysics is critically important for the understanding of the molecular nature of nucleation phenomena. While the structural and thermochemical properties of hydrogen-bonded complexes of simple, common acid with water are of considerable importance for fundamental physics and chemistry, the polarity of complexes being formed is important with regards to a number of environmental issues.^{5–21}

The importance of the precise location of the most stable isomers (global minima) and accurate description of their properties is obvious. Typically, experiments are able to trace the most stable isomer at low temperatures. However, gas consisting of clusters of exactly same chemical identity is not uniform. Less stable, yet equilibrium isomers (local minima) may also contribute to the gas composition. Because the Gibbs free energy controlling the cluster stability is temperature-dependent and cluster entropies may be unequal, different isomers may serve as global minima at different temperatures. Another important detail is that at elevated temperatures the inverse temperature dependence of the exponent in the Boltz-

* Corresponding author. E-mail: alexn@asrc.cestm.albany.edu.

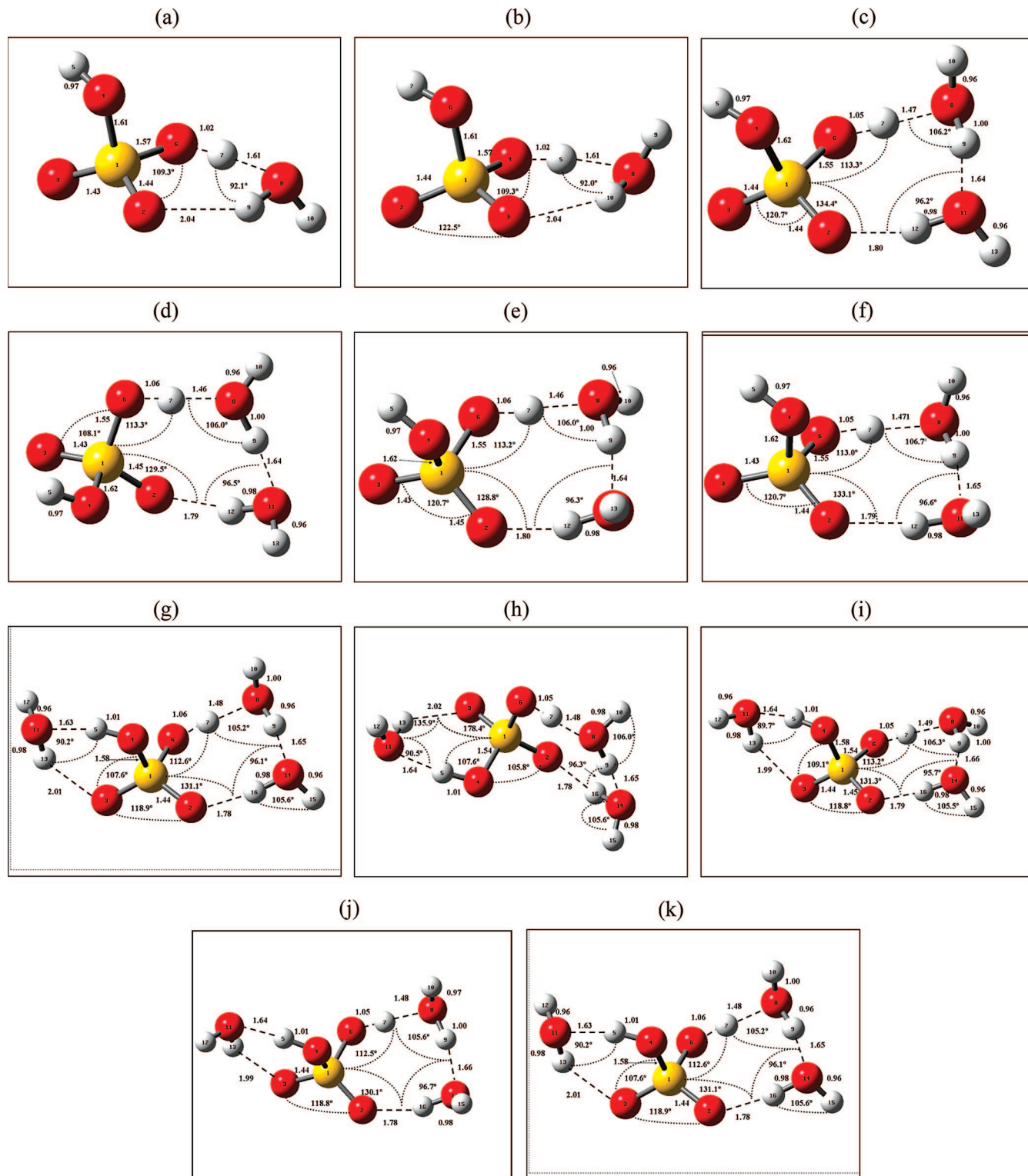


Figure 1. Optimized geometries of the global minima and neighboring local minima for SW-I (a), SW-II (b), SW2-I (c), SW2-II (d), SW2-III (e), SW2-IV (f), SW3-I (g), SW3-II (h), SW3-III (i), SW3-IV (j), and SW3-V (k) obtained at the PW91PW91/6-311++G(3df,3pd) level of theory.

mann partition function may suppresses the domination of single global minimum broadening the cluster spectrum.

In the present paper, the structure, stability, and electrical dipole moments of sulfuric acid hydrates have been investigated using quantum methods. The aforementioned clusters have been studied using density functional theory, ab initio MP2 and G3 model chemistry methods.

2. Methods

G3 theory has been developed by Curtiss and Pople with co-workers to predict highly accurate energies and has been tested on hundreds of species. Ab initio second-order Moller–Plesset perturbation theory (MP2) commonly used in the computational practice comprises good predictivity with reasonable computational costs. B3LYP, which is the most commonly used density

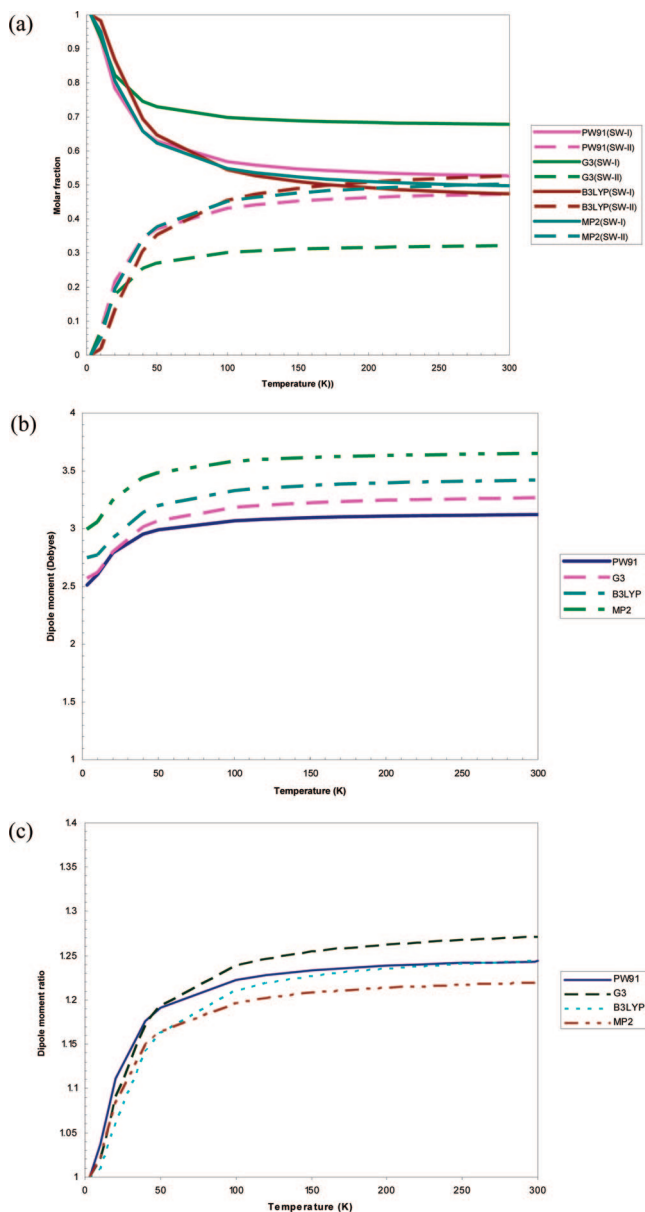


Figure 2. Comparison of the (a) temperature-dependent isomer fractions, (b) Boltzmann–Gibbs average dipole moment of $(\text{H}_2\text{SO}_4)(\text{H}_2\text{O})$ isomer mixture, and (c) ratio of Boltzmann–Gibbs average dipole moment to the dipole moment of most stable isomer calculated at PW91PW91/6-311++G(3df,3pd), B3LYP/6-311++G(3df,3pd), MP2/6-311++G(2d,2p), and G3 levels of theory.

functional, and PW91PW91, which is able to predict the cluster thermochemistry in good agreement with experiments,^{11,15,21,24–26} have been selected for the DFT calculations. Another important factor that convinces us to choose the specific DFT methods is their ability to reproduce geometries and dipole moments of a number of molecules/clusters, including H_2SO_4 , and H_2O , with quite high accuracy.^{11,19} To minimize uncertainties associated

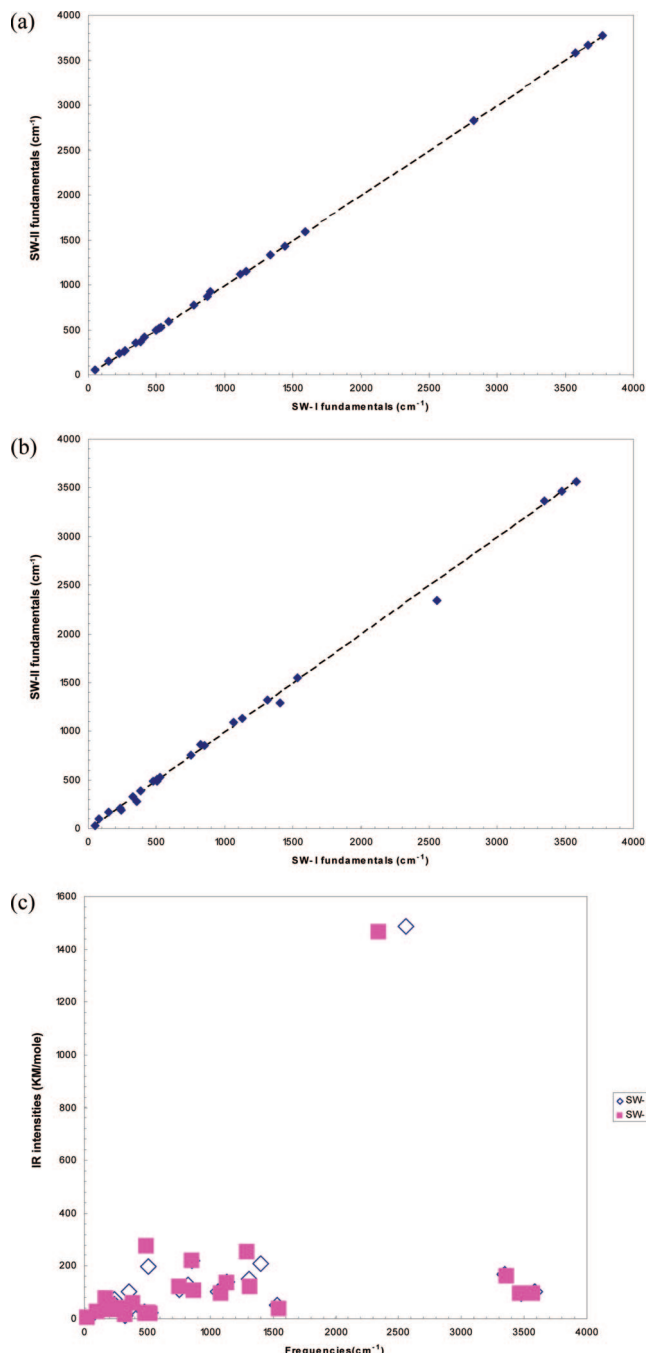


Figure 3. Comparison of (a) harmonic spectra and (b) anharmonic spectra. (c) IR intensities of isomers SW-I and SW-II of $(\text{H}_2\text{SO}_4)(\text{H}_2\text{O})$ calculated at PW91PW91/6-311++G(3df,3pd) levels of theory.

with the basis set superposition error, most of MP2 and DFT calculations have been carried out using large Pople basis sets 6-311++G(3df,3pd) (DFT) and 6-311++G(2d,2p). Because structures of $(\text{H}_2\text{SO}_4)(\text{H}_2\text{O})_n$ have been studied in some detail in the past, equilibrium geometries obtained in refs 19–23 and

TABLE 1: Dipole Moments (Debyes) of Sulfuric Acid Hydrates $(\text{H}_2\text{SO}_4)(\text{H}_2\text{O})_n$ ($n = 1–3$)^a

	SW-I	SW-II	SW2-I	SW2-II	SW2-III	SW2-IV	SW3-I	SW3-II	SW3-III	SW3-IV	SW3-V
PW91	2.51 (0.0)	3.8 (0.06)	3.35 (0.0)	2.64 (0.037)	3.6 (0.067)	5.03 (0.4)	2.86 (0.0)	2.96 (0.06)	4.163 3(0.37)	2.95 (0.51)	1.125 (0.73)
B3LYP	2.75 (0.06)	4.0 (0.0)	3.30 (0.07)	3.54 (0.0)	3.30 (0.06)	4.86 (0.44)	2.74 (0.0)	2.936 (0.01)	3.98 (0.05)	2.90 (0.45)	0.75 (0.74)
G3 ^b	2.57 (0.0)	4.09 (0.09)	3.12 (0.0)	3.00 (0.23)	3.01 (0.24)	4.62 (0.44)	2.65 (0.0)	2.69 (0.16)	3.26 (0.24)	3.00 (0.26)	1.04 (0.15)
MP2	2.99 (0.0)	4.3 (0.01)									

^a The difference in the free energy (kcal mol⁻¹) from the most stable isomer of the class is given in parentheses. ^b Geometry optimization at the MP2/6-31+G* level.

TABLE 2: Comparison of Fundamentals (cm⁻¹) and the Difference between Them Δ (%) for Most Stable Isomers of Sulfuric Acid Monohydrate SW-I and SW-II Computed Using PW91, B3LYP, and G3

mode	PW91			B3LYP			G3 ^a		
	SW-I	SW-II	Δ(%)	SW-I	SW-II	Δ(%)	SW-I	SW-II	Δ(%)
1	3769.6	3770.6	-0.03	3874.0	3874.9	-0.02	4158.9	4159.9	0.0
2	3668.1	3667.2	0.02	3774.2	3774.0	0.01	4041.0	4042.4	0.0
3	3575.9	3572.6	0.09	3733.4	3737.1	-0.10	4038.9	4039.3	0.0
4	2827.0	2833.2	-0.22	3131.9	3138.0	-0.19	3637.6	3650.6	-0.4
5	1594.2	1595.1	-0.05	1627.7	1627.7	0.00	1823.4	1824.0	0.0
6	1444.0	1431.6	0.86	1466.5	1461.8	0.32	1583.0	1580.0	0.2
7	1337.7	1326.6	0.83	1361.5	1348.6	0.95	1456.0	1440.9	1.0
8	1155.4	1154.9	0.05	1204.0	1204.2	-0.02	1309.3	1310.0	-0.1
9	1116.5	1115.6	0.08	1152.8	1153.7	-0.08	1293.0	1295.3	-0.2
10	893.6	922.3	-3.21	909.1	909.7	-0.06	1028.0	1026.8	0.1
11	871.0	869.0	0.23	843.4	866.4	-2.72	946.0	943.9	0.2
12	775.7	770.8	0.63	818.3	816.8	0.19	808.6	851.9	-5.3
13	589.0	591.1	-0.36	562.9	560.1	0.51	614.4	612.8	0.3
14	533.9	531.5	0.45	555.1	547.0	1.47	606.5	605.8	0.1
15	517.6	518.0	-0.07	540.4	536.0	0.81	566.9	562.2	0.8
16	494.3	496.6	-0.48	503.1	506.7	-0.72	519.2	521.2	-0.4
17	415.4	417.5	-0.51	429.2	431.3	-0.48	460.6	462.9	-0.5
18	383.6	366.7	4.40	379.0	372.4	1.74	411.7	410.7	0.2
19	349.1	353.6	-1.29	353.2	336.9	4.62	351.0	333.7	4.9
20	267.2	265.8	0.51	264.8	263.1	0.62	281.8	280.4	0.5
21	260.1	262.5	-0.89	240.0	225.8	5.94	224.2	227.4	-1.4
22	227.7	231.9	-1.84	222.1	224.4	-1.03	186.7	188.1	-0.8
23	149.9	150.7	-0.54	131.2	125.2	4.58	124.8	124.8	0.0
24	50.1	48.4	3.49	50.8	46.2	9.08	48.4	46.0	5.0

^a Geometry optimization at the MP2/6-31+G* level.**TABLE 3: Comparison of Rotational Constants (GHz) and the Difference between Them Δ (%) for Most Stable Isomers of Sulfuric Acid Monohydrate SW-I and SW-II Computed Using PW91, B3LYP, and G3**

method	SW-I	SW-II	Δ (%)
PW91	4.917	4.894	0.46
	1.922	1.934	-0.62
	1.890	1.902	-0.66
	4.999	5.014	-0.30
B3LYP	1.892	1.892	0.03
	1.867	1.865	0.09
	5.088	5.120	-0.63
G3	1.871	1.848	1.22
	1.855	1.830	1.36

27 have been used in the present study as some of the initial guess geometries. One or more local minima with the Gibbs free energy close to that of the most stable isomer have been located in the immediate (~ 0.5 – 0.7 kcal mol⁻¹) vicinity of each global minimum.

3. Results and Discussion

Figure 1 presents optimized geometries of the global minima and neighboring local minima for (H₂SO₄)(H₂O)_n ($n = 1, 2, 3$) and Table 1 presents dipole moments of these clusters.

As seen from Table 1, isomers of nearly identical stability and spectral characteristics have drastically different dipole moments. The difference in the dipole moment of mono-, di-, and trihydrates of the sulfuric acid exceeds 1.3–1.5 Debyes (~ 50 – 60%), 1.4–2.6 Debyes (~ 50 – 90%), and 3.8–4.2 Debyes (~ 370 – 550%), respectively.

The isomer SW-I detected and described in great detail in low-temperature matrix and gas-phase experiments has been identified as the global minimum at low temperatures by all methods. B3LYP predicts SW-II to be more stable than SW-I at 298.15 K; however, at low temperatures SW-I becomes a

dominant (see Figure 2). SW-II located $< \sim 0.1$ kcal mol⁻¹ above the global minimum has a remarkably similar structure, with virtually identical O–O distances and HOH and OHO angles within the hydrogen-bonded network.

A similar pattern was observed for di- and trihydrates in nearly all the cases studied here. For example, the difference in the aforementioned distances and angles between the five most stable isomers of (H₂SO₄)(H₂O)₃ located within ~ 0.7 kcal mol⁻¹ of the global minima does not exceed 0.1 and 0.4%, respectively. The only visible dissimilarity found in the structures of global and local minima of nearly identical stability is the orientation of free hydrogen bonds.

Figure 2 presents a comparison of (a) the temperature-dependent isomer fractions, (b) the Boltzmann–Gibbs average dipole moment of (H₂SO₄)(H₂O) isomer mixture, and (c) the ratio of Boltzmann–Gibbs average dipole moment to the dipole moment of most stable isomer calculated at PW91PW91/6-311++G(3df,3pd), B3LYP/6-311++G(3df,3pd), MP2/6-311++G(2d,2p), and G3 levels of theory.

As seen from Figure 2, the strong temperature dependence of the isomer concentrations coupled with the difference in the dipole moment of low laying isomers of nearly identical stability lead to large variations in the Boltzmann–Gibbs average for dipole moments. A comparison of curves in Figure 3 shows clearly that under atmospheric conditions the dipole moment of the global minimum measured at low temperatures may not be representative. Aforementioned variations have a direct impact on the dipole–charge interaction and the ability of the ions to attract and accommodate the pre-existing sulfate clusters.

In the last decades, advanced experimental techniques for measuring structures and dipole moments have been developed. However, the derivation of experimental structures and dipole moment involves substantial theoretical and computational efforts. While rotational constants are used in the evaluation experimental data for both structure and dipole moment measurements, vibrational spectra and absorption intensities

serve as “fingerprints” to identify a known molecule, or reveal the geometry of one that has not been characterized before. Tables 2 and 3 present a comparison of vibrational spectrums and rotational constants of most stable isomers of sulfuric acid monohydrate SW-I and SW-II, respectively. As seen from Table 2, the vibrational spectrums of SW-I and SW-II are very similar, and the average difference between fundamentals does not exceed a fraction of percent. As seen from Table 3, the rotational constants of SW-I and SW-II are also very close. A similar pattern was observed for di- and tri-hydrates in nearly all the cases studied here.

The present spectroscopic analysis shows that in nearly all cases global minima and neighboring local minima have nearly identical spectral characteristics, very close rotational constants, and absolute entropies. Being unable to find distinct features in harmonic spectra of isomers of close stability, we decided to explore the anharmonic correction. As seen from Figure 3a, the application of anharmonic correction leads to some dissimilarity in SW-I and SW-II spectra, particularly in the location of the strong adsorption peak.

4. Conclusion

In the paper, common atmospheric $\text{H}_2\text{SO}_4\text{--H}_2\text{O}$ complexes have been studied using DFT, G3 model chemistry and MP2 methods. The present work leads us to the following conclusions:

(a) The immediate vicinity of the global minima is populated with a number of local of nearly identical spectral characteristics and rotational constants, and drastically (by up to 550 %) different dipole moments.

(b) Under the atmospheric conditions ($T = 200\text{--}300\text{ K}$) the strong temperature dependence of isomer concentrations coupled with the drastic difference in the dipole moment between global and local minima of nearly identical stability may lead to the large difference between the Boltzmann–Gibbs average and dipole moment of the global minima. This implies that under

atmospheric conditions the dipole moment of global minima measured at low temperatures may not be representative.

References and Notes

- (1) Charlson, R. J. *Science* **1992**, 255, 423.
- (2) Riipinen, I. *Atmos. Chem. Phys.* **2007**, 7, 1899–1914.
- (3) Laakso, L. *Atmos. Chem. Phys.* **2007**, 7, 1333.
- (4) Hirsikko, A. *Atmos. Chem. Phys.* **2007**, 7, 201.
- (5) Yu, F.; Z.; Wang, G.; Luo, R. P.; Turco, *Atmos. Chem. Phys. Discuss.* **2007a**, 7, 13597.
- (6) Yu, F.; Z.; Wang, G.; Luo, R. P.; Turco, *Atmos. Chem. Phys. Discuss.* **2007b**, 7, S6754.
- (7) Arnold, F. *Nature* **1980**, 284, 610–611.
- (8) Yu, F.; Turco, R. P. *Geophys. Res. Lett.* **2000**, 27, 883.
- (9) Nadykto, A. B.; Yu, F. *J. Geophys. Res.* **2003**, 23, doi:10.1029/2003JD003664.
- (10) Nadykto, A. B.; Yu, F. *Phys. Rev. Lett.* **2004**, 93, 016101.
- (11) Nadykto, A. B. et al. *Phys. Rev. Lett.* **2006**, 96, 125701.
- (12) Castleman, A. W. J.; Tang, I. N. *J. Chem. Phys.* **1972**, 57, 3629–3638.
- (13) Knaapen, M.; Borm, P. J.; Albrecht, C.; Schins, R. P. *Int. J. Cancer* **2004**, 109, 799.
- (14) Saxon, D.; Diaz-Sanchez, D. *Nature Immunol.* **2005**, 6 (3), 223.
- (15) Fiacco, D. L.; Hunt, S. W.; Leopold, K. R. *J. Am. Chem. Soc.* **2002**, 124 (16), 4504.
- (16) Couling, S. B. *Phys. Chem. Chem. Phys.* **2003**, 5, 4108.
- (17) Couling, S. B. *J. Am. Chem. Soc.* **2003**, 125 (43), 13038.
- (18) Hanson, D. R.; Eisele, F. *J. Phys. Chem. A* **2000**, 104 (8), 1715.
- (19) Al Natsheh, A. et al. *J. Phys. Chem. A* **2004**, 108 (41), 8914.
- (20) Brauer, C. S.; Sedo, G.; Leopold, K. R. *Geophys. Res. Lett.* **2006**, 33, L23805, doi:10.1029/2006GL028110.
- (21) Nadykto, A. B.; Yu, F. *Chem. Phys. Lett.* **2007**, 1–3, 14.
- (22) Bandy, A. R.; Ianni, J. C. *J. Phys. Chem. A* **1998**, 102 (32), 6533.
- (23) Ianni, J. C.; Bandy, A. R. *J. Mol. Struct. (THEOCHEM)* **2000**, 497, 19.
- (24) Tsuzuki, S.; Lüthi, H. P. *J. Chem. Phys.* **2001**, 114, 3949.
- (25) Kurten, T. et al. *J. Phys. Chem. A* **2006**, 110, 7178.
- (26) Kurten, T.; et al. *J. Geophys. Res.* **2007**, 112, D4, D04210, 10.1029/2006JD007391.
- (27) Re, S.; Osamura, Y.; Morokuma, M. *J. Phys. Chem. A* **1999**, 103, 3535.

JP711803R